Hybrid Approaches Towards 3D Concrete Printing for Lightweight Reinforced Concrete Structures

Mania Aghaei Meibodi[1], Yuxin Lin[1], Hao Chen[1]

DART Laboratory, Taubman College, University of Michigan, Ann Arbor, MI 48109, USA
meibodi@umich.edu

Abstract. 3D Concrete Printing (3DCP) has paid little attention to producing material-efficient parts. Material optimization methods, such as topology optimization, often result in forms with complex geometries—extreme overhangs and multi-branching—that are challenging to achieve in large-scale 3DCP. The limited studies on 3DCP of topology-optimized forms often (a) use excessive supporting material, resulting in waste, or (b) discretize topology-optimized forms into simpler components that are later assembled, leading to labor-intensive assembly and accuracy errors. This research seeks to enable the 3D concrete printing of such structures in a streamlined process, eliminating the need for discretization and support materials. To prevent collapse during the 3D printing of extreme overhangs, we explore a method that combines 3DCP with the simultaneous casting of fast-setting concrete materials. For precise concrete deposition that accurately follows the contours of a shape, we introduce topology-informed non-planar printpath and a variable material deposition rate. The method is investigated through a construction scale load-bearing wall, Branch Wall, with steep cantilever branches and in-between thin surfaces and a series of S-Shape specimens (230 mm diameter and 500 mm height) produced through simultaneous 3DCP and casting of fast-setting concrete.

Keywords: 3D Concrete Printing, Topology Optimization, Complex Geometries, Sequential Casting of Set on Demand Concrete.

1 Introduction: 3D Concrete Printing for Prefabrication of Materially Optimized Building Components

Reinforced concrete (RC) enables the construction of essential long-span, large, multi-story infrastructure for urban densification, thus vital for projected rapid urbanization [1]. A significant concern arises from the inefficient utilization of concrete, making it the second most consumed substance worldwide [2]. Creating structurally efficient forms that minimize material usage often necessitates the use of bespoke formwork, which can incur high costs, sometimes exceeding 50% of the allocated budgets for the entire structure [3]. 3D Concrete Printing (3DCP), as a method of shaping concrete without the need for formwork [4], has the potential to enable the creation of materially optimized structural parts.

https://doi.org/10.24355/dbbs.084-202408140649-0

However, for over two decades, 3DCP has focused on single-family homes with thick, unreinforced walls that use more concrete and cement than traditional formwork-based concrete structures. The utilized technology, often based on Contour Crafting [5], involves a CNC machine that prints concrete layer-by-layer along a planar path. This results in a permanent formwork filled with rebar and concrete. Yet, achieving materially optimized forms with planar 3DCP (P-3DCP) is challenging due to their inherent complex geometries such as sharp cantilevered branches and surfaces, that often require additional supports to prevent collapse during 3D printing (Fig. 1e). These supports can lead to material waste, as seen in the Krypton column and OptiBridge projects [6,7], where extra scaffolding was necessary during the 3D printing and was removed in post-processing steps (Fig. 1a, b). Another approach to mitigate this complexity was presented in the optimal concrete girder project [8], where a complex topology-optimized form had to be divided into smaller simple components to satisfy planar 3D printability, additionally, each part was encased by sand to support the overhangs. Subsequently, the final structure was assembled by post-tensioning of its many parts with imprecise segment interfaces, risking reduced structural integrity and inaccurate assembly alignment (Fig. 1d). There is limited research on approaches toward 3DCP that enable the efficient fabrication of lightweight or material-optimized structural building elements.

Fig. 1. Limitations of P-3DCP for optimized structures: (a & b) OptiBridge and XtreeE projects requiring extra scaffolding surfaces during 3D printing to support extreme overhangs that are later removed; (c) post-processed XtreeE column; (d) misalignment in assembling multiple simplified parts of the Girder beam; (e) inherent staircase effect in P-3DCP.

2 Method: Coupling Non-Planar Robotic 3DCP with Sequential Casting of Set on Demand Concrete

While 3D printing can effectively produce small-scale, materially optimized parts like car components using planar toolpaths and additional supports, this approach is not efficient for building elements. Given the larger scale and the speed required for constructing such structures, this approach leads to substantial material waste and increased fabrication time. To achieve the manufacturing of lightweight structural building elements, without support material and excessive discretization, this research develops the following methods:

A topology-informed non-planar printpath (NP-Path) and variable material deposition rate guided by the NP-Path for precise concrete deposition along the contours of complex shapes. To prevent overhang failure during printing, our method involves simultaneous non-planar 3D Concrete Printing (NP-3DCP) and casting of fast-setting

https://doi.org/10.24355/dbbs.084-202408140649-0

material. While NP-Path addresses some issues, sharp tubular overhangs such as those from topology optimization may still collapse. These areas risk failure under their own weight without support or an immediate material setting. Here, the cast fast-setting concrete takes its shape from the 3D-printed concrete formwork and, at the same time, shores the 3D-printed formwork because of its fast-setting time. In the areas where reinforcement is needed such as structural ribs, the following two scenarios or their hybrid are proposed:

- First, 3D printing of the non-planar stay-in-place formwork (SP-formwork), followed by sequential rebar integration and sequential concrete casting.
- 3D printing a reinforcement conduit as part of the Non-Planar SP-formwork for the post-integration of tensile elements such as tensile wire.

Version one of the methods was tested through a 1:1 scale prototyping of a topologically optimized reinforced structural wall, and version two, which evolved from lessons learned from the 1:1 scale prototype, was examined through a series of S-shaped specimens representing complex rib scenarios in a materially optimized form. Using normal-setting concrete and a 1K 3DCP system to create SP-formwork, these methods were evaluated, assessing the worst-case scenario. Unlike two components (2K) 3DCP, where an accelerator is mixed with the concrete at the end-effector to reduce the setting time of the 3D printed formwork, one component (1K) 3DCP uses a standard concrete mix that sets more slowly, significantly increasing the risk of collapse after several layers. The 1k 3DCP system is more affordable and accessible than the 2k system which requires proprietary material, but minimal research is done on creating complex geometries without extensive support [9]. The following sections will explore the potential of this method for complex geometries and will highlight the challenges learned in the process that should be addressed to efficiently 3DCP lightweight structural elements.

3 Non-Planar Printpath and Variable Material Deposition for 3DCP of Complex Geometries

NP-Path and variable material deposition are essential for accurately following the intricate shapes of topology-optimized structures (Fig. 2a, b). NP-3DCP allows for adjustable orientations and layer heights to model complex 3D geometries precisely (Fig. 2e, f), necessitating the use of robotic arms with 6 degrees of freedom. While robotic Non-planar 3D printing in plastics has significantly enhanced scaffolding-free construction, surface quality, and mechanical integrity [10], research on NP-3DCP remains limited [11]. Regardless of the method used to generate NP-Path, the layer heights must be adjusted to fit within the maximum and minimum height capacities of the 3DCP system. A computational model was developed that automatically adjusts the material deposition rate in accordance with the variation in height difference between two layers being 3D printed using a simple equation Eq. (1).

https://doi.org/10.24355/dbbs.084-202408140649-0

$$H * W = F / V \tag{1}$$

H = filament height; W = extrudate material width; F = material flow rate based on pump speed; V = robot print speed. Varying material deposition rates across the NP-Path can be achieved through varying F or V. The conducted tests suggest that varying V while keeping the F constant provides more control over the process and eliminates unstable material deposition that negatively impacts buildability. The main challenge lies in accounting for the uneven deformation of concrete filaments as a result of the weight of subsequent layers and shrinkage. Integrating these factors into the computational design of printpath is more complex in NP-3DCP due to the constantly changing geometry. This requires enhanced data collection and real-time adaptation of the NP-Path.

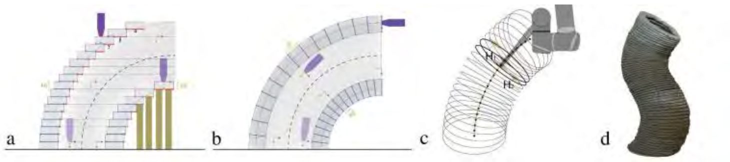

Fig. 2. a) Planar 3DCP requiring external supports (yellow) for overhangs. b) NP-Path, slicing shapes along contours but requiring 6-axis freedom to tilt the end effector. c) A method of generating varying heights in NP-Path and remapping them to the possible domain of concrete filament thickness. d) S-shape prototype showing the variation of height across a layer.

4 Non-Planar 3DCP and Sequential Rebar Integration and Sequential Casting of Fast Setting Concrete

"Branch Wall" load-bearing structure, sized 1.2 x 2 meters, was created using computational topology optimization. It features an elaborate rib layout with a 30-degree overhang and thin membranes between the ribs, aligned with internal force paths from six load points and three supports (Fig. 3a). These ribs are translated into an SP-formwork system, which supports rebar encased in 25-35mm of concrete, optimizing material usage around the rebar (Fig. 3b). To optimize the integration of rebar into the 3D printing process, the ribs were simplified into more linear trajectories, which helps in incorporating longitudinal rebar more efficiently without the need to segment them into smaller pieces (Fig. 3c). A simple NP-Path that enables 3DCP along the contour of geometry was generated to direct the end effector for variable material deposition. Two prototypes were fabricated based on this design, one that was intended for 3DCP the entire structure then integrating rebar and casting it, and one that would involve interrupted integration of rebar and sequential casting. However, branches with extreme overhangs (30 degrees), although not problematic during the printing process, were susceptible to collapse from their own weight once they reached a certain height from the bifurcation point (approximately 50cm). This was because the bonding strength at the layers located at bifurcation was not strong enough to overcome the moment force as the height of the branch increased. The increased weight of the branch can lead to

https://doi.org/10.24355/dbbs.084-202408140649-0

delamination of the interlayers over time, weakening structural integrity (Fig. 3d). To address this, simultaneously a second prototype (Fig. 4a) was successfully fabricated incorporating the casting of set-on-demand concrete (fast-setting) with sequential rebar reinforcement at every 50cm (Fig. 4b, c, d).

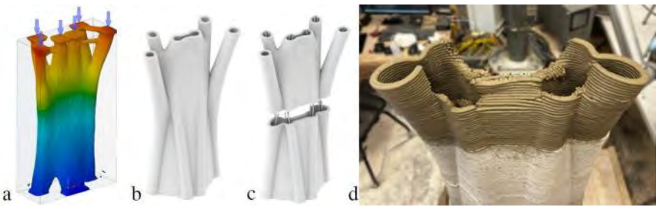

Fig. 3. a) Topology optimization for 6-load/3-support setup; b) SP-formwork design for rebar and concrete casting; c) post-rationalization of rebar integration; d) Initial 3DCP SP-formwork prototype failure at branched regions due to moment force.

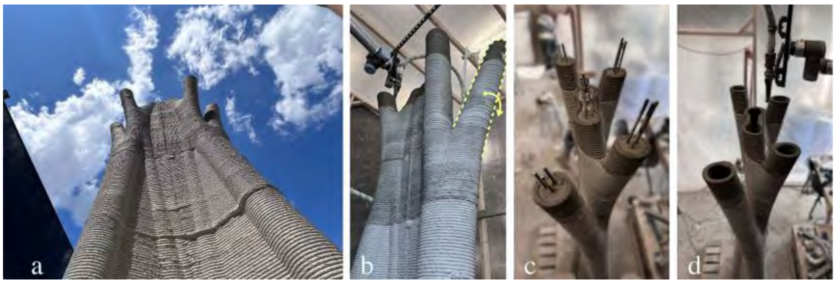

Fig. 4. This image shows the 3DCP with sequential rebar integration and casting of the second prototype and highlights the successful branches that collapsed in the previous prototype.

5 3DCP of Stay-in-Place Formwork with Reinforcement Conduit and Sequential Casting of Fast-Setting Material

To expand methods for manufacturing complex geometries, we explored NP-3DCP and sequential casting of quick-setting concrete, while 3D printing cavities for later post-tension element placement. To investigate the feasibility of this method, an S-shaped structure featuring internal reinforcement conduits was designed. 50 non-planar layers with heights ranging from 6.5mm to 17.2mm, guided the continuous adjustments of the toolhead tilt angle from 0 to 40 degrees relative to the Z-axis (Fig. 5d). we investigated how many layers can be 3D printed before casting and how high casting can happen to eliminate deformation of 3DCP SP-formwork under hydrostatic pressure. For our material described in section 6, every 20 layers of NP-3DCP would need 10 cm height (approximately 10 layers) of cast fast-setting material (Fig. 5b). To allow the lower layers to gain sufficient stiffness, 5cm of height was cast in the first 15 layers (Fig. 5a). In the areas where the layer height and overhanging angle were at their maximum, any delay in sequential casting resulted in observed deformation (Fig. 5c). Early tests

https://doi.org/10.24355/dbbs.084-202408140649-0

identified two challenges: determining the optimal ambient temperature for increased buildability before casting and finding each ideal concrete material rheology for 3DCP of SP-formwork and casting.

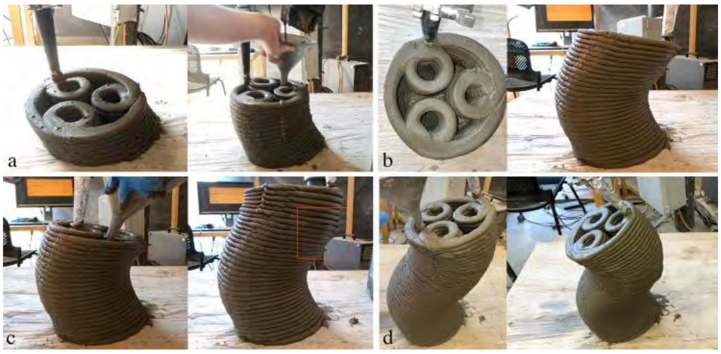

Fig. 5. a) Initial casting after 15 layers of concrete printing; b) 10cm height of casted fast-setting material for every 20 layers of NP-3DCP; c) deformation observed due to delay in sequential casting; d) successful printing of the S-shape part.

6 Temperature Control for Increasing Buildability in 3D Concrete Printing

Higher temperatures of both the layer surfaces and the surrounding environment can significantly decrease the initial setting time of extruded concrete [13], helping in buildability. We used this approach for 3DCP of complex geometries with a one-component (1k) system, which generally builds limited early strength. To determine the optimal temperature requirements for achieving sufficient early strength, we conducted comparative tests at three different temperature settings: room temperature (22°C), and heated ambient temperature (29.4°C) on a similar shape with a planar path. Maintaining a heated ambient temperature of approximately 29.4°C, which resulted in layer surface temperatures between 23.9-25.6°C, proved effective for the continuous 3DCP of up to 35 layers with variable layer heights in the Z-axis (Fig. 6a, b). Conversely, experiments conducted at room temperature (22°C) showcased layer deformations after 10 layers (Fig. 6c).

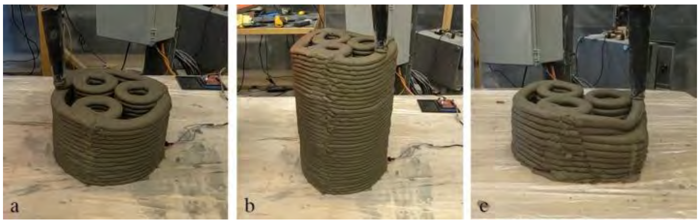

Fig. 6. a, b) Heating the environment to 29.4°C ensured stable 3DCP for at least 35 layers; c) deformations occurred during 3DCP at room temperature after 10 layers.

https://doi.org/10.24355/dbbs.084-202408140649-0

7 Material Composition for 3DCP and Fast Setting Concrete Material for Sequential Casting

Two different mortars were prepared for 3DCP and casting due to different process-related rheological requirements. 3DCP mortar possesses a high yield stress for shape retention and buildability, whereas casting mortar possesses a low viscosity for excellent formwork-filling. The 3DCP mortar comprises ASTM Type I OPC from Quickcrete, Boral Micron3 fly ash, fine silica sand of sizes 0.2-0.6mm, and superplasticizer. The water-to-cement ratio, water-to-binder ratio, and sand-to-binder ratio were set at 0.65, 0.33, and 0.35, respectively. Additionally, 0.19 % of superplasticizer, relative to the binder, is included. The casting mortar uses a fast-setting cement from Quickcrete, characterized by an initial setting time of 10 minutes, with a w/c ratio of 0.14.

Rheological properties (i.e., plastic viscosity, μ and static yield stress, τ_s) were measured using an ICAR Plus rheometer, equipped with a coaxial cylinder having an inner radius of 100 mm and a four-blade vane geometry with a radius of 63.5 mm and a height of 127 mm. The flow curve test protocol involved pre-shearing at 30 rpm for 20 s; followed by actual shearing at an initial speed of 30 rpm and final speed of 0.6 rpm, with data captured at 24 distinct points, each for 5 s. The stress growth test protocol involved pre-shearing at 30 rpm for 20 s; followed by a rest period of 2 minutes; and then continued at 30 rpm until peak stress was reached. The μ and τs of 3DCP mortar were tested at ages 15, 30, 45, and 60 minutes after mixing with water, and the μ of casting mortar was tested at ages 5, 10, and 15 mins. The intervals were selected according to the printing process (i.e., extrusion started 30 mins after mixing with water, which includes the mixing, resting, and pumping, and took 30 minutes for printing) and the sequential casting process (i.e., casting started 5 mins after mixing with water) for one batch of the material.

Fig. 7 presents the results of rheological tests. For 3DCP mortar, the μ values were relatively constant below 20 Pa•s at 60 mins, whereas the τ_s values increased gradually from 277 Pa at 15 mins to 457 Pa at 60 mins. In the case of cast mortar, the μ value increases sharply from 41.9 Pa•s at 5 mins to 190.4 Ps•s at 15 mins.

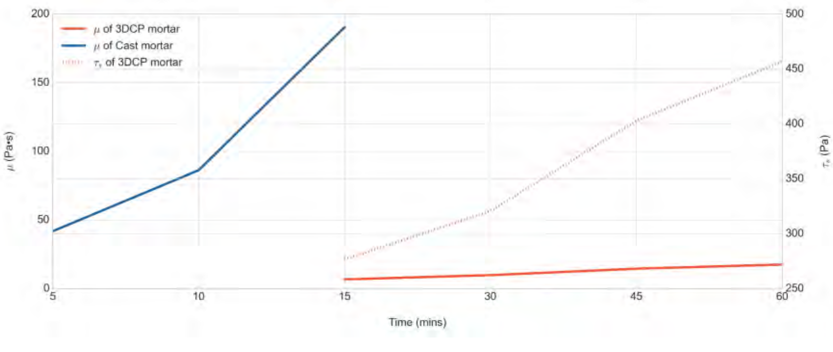

Fig. 7. The evolutions of plastic viscosity and static yield stress of 3DCP mortar and cast mortar at different ages.

https://doi.org/10.24355/dbbs.084-202408140649-0

8 Conclusion

The proposed method of NP-3DCP and sequential casting of fast-setting concrete expand the application of 1K 3DCP for the fabrication of complex geometries with overhang branching without discretization and support material, a hybrid of non-planar 3DCP and sequential casting of fast-setting concrete. Using this method, a topology optimized reinforced structure entailing branches up to 790 mm with 70-degree overhangs was successfully fabricated. The Branch Wall weighs 367 kg with load bearing capacity of 25 MPa, achieving a 68% material reduction compared to traditional concrete walls, and a 76.4% reduction compared to standard 3DCP walls. Investigating the bond strength between 3DCP stay-in-place formwork and the cast will enhance our understanding of the formwork's structural role.

References

1. Van Damme, H. Concrete material science: Past, present, and future innovations. Cement and Concrete Research, 112, 5–24 (2018).
2. Kloft, H., Empelmann, M., Hack, N., Herrmann, E., & Lowke, D. Reinforcement strategies for3D-concrete-printing. (2020).
3. García De Soto B Productivity of digital fabrication in construction: Cost and time analysis of a robotically built wall. (n.d.). Automation in Construction, 92, 297–311.
4. Wangler, T., Lloret, E., Reiter, L., Hack, N., Gramazio, F., Kohler, M., Bernhard, M., Dillenburger, B., Buchli, J., Roussel, N., & Flatt, R. Digital Concrete: Opportunities and Challenges. RILEM Technical Letters, 1, 67–75 (2016).
5. Khoshnevis, B. Automated construction by contour crafting - Related robotics and information technologies. Automation in Construction, 13, 5–19 (2004).
6. Gaudillière, N., Duballet, R., Bouyssou, C., Mallet, A., Roux, P., Zakeri, M., & Dirrenberger, J. Large-scale additive manufacturing of ultra-high-performance concrete of integrated formwork for truss-shaped pillars. In Robotic Fabrication in Architecture, Art and Design, pp. 459–472. Springer International Publishing (2019).
7. Ooms, T., Vantyghem, G., Tao, Y., Bekaert, M., De Schutter, G., Van Tittelboom, K., & De Corte, W. The production of a topology-optimized 3D-printed concrete bridge. In RILEM Bookseries, pp. 37–42. Springer International Publishing (2022).
8. Vantyghem, G., De Corte, W., Shakour, E., & Amir, O. 3D printing of a post-tensioned concrete girder designed by topology optimization. Automation in Construction (2020).
9. Kamhawi, A., & Aghaei Meibodi, M. (2024). Extrusion based 3D concrete printing, Complex geometries in 3D concrete printing, 3D Printing parameters. The Journal of Automation in Construction, Manuscript No. AUTCON-D-24-00873.
10. Mitropoulou, I., Bernhard, M., & Dillenburger, B. Nonplanar 3D printing of bifurcating forms. 3D Printing and Additive Manufacturing, 9(3), 189–202 (2022).
11. Bhooshan, S., Bhooshan, V., Megens, J., Casucci, T., Van Mele, T., & Block, P. Print-path design for inclined-plane robotic 3D printing of unreinforced concrete. In Towards Radical Regeneration (pp. 188–197). Springer International Publishing (2023).
12. Psu.edu, https://www.engr.psu.edu/ce/courses/ce584/concrete/library/materials/Admixture/Link-settime.htm, retrieved April 15, 2024.

https://doi.org/10.24355/dbbs.084-202408140649-0